Original Article

Rat liver extracellular matrix and perfusion bioreactor culture promote human amnion epithelial cell differentiation towards hepatocyte-like cells

Journal of Tissue Engineering
Volume 14: 1–17

DOI: 10.1177/20417314231219813
journals.sagepub.com/home/tej
Sage

Sara Campinoti[1,2], Bruna Almeida[1,2], Negin Goudarzi[1,2], Stefan Bencina[3], Fabio Grundland Freile[1,4], Claire McQuitty[1,2], Dipa Natarajan[1,2], I Jane Cox[1,2], Adrien Le Guennec[5], Vamakshi Khati[6], Giulia Gaudenzi[7], Roberto Gramignoli[3,8*] and Luca Urbani[1,2*]

Abstract

Congenital and chronic liver diseases have a substantial health burden worldwide. The most effective treatment available for these patients is whole organ transplantation; however, due to the severely limited supply of donor livers and the side effects associated with the immunosuppressive regimen required to accept allograft, the mortality rate in patients with end-stage liver disease is annually rising. Stem cell-based therapy aims to provide alternative treatments by either cell transplantation or bioengineered construct transplantation. Human amnion epithelial cells (AEC) are a widely available, ethically neutral source of cells with the plasticity and potential of multipotent stem cells and immunomodulatory properties of perinatal cells. AEC have been proven to be able to achieve functional improvement towards hepatocyte-like cells, capable of rescuing animals with metabolic disorders; however, they showed limited metabolic activities in vitro. Decellularised extracellular matrix (ECM) scaffolds have gained recognition as adjunct biological support. Decellularised scaffolds maintain native ECM components and the 3D architecture instrumental of the organ, necessary to support cells' maturation and function. We combined ECM-scaffold technology with primary human AEC, which we demonstrated being equipped with essential ECM-adhesion proteins, and evaluated the effects on AEC differentiation into functional hepatocyte-like cells (HLC). This novel approach included the use of a custom 4D bioreactor to provide constant oxygenation and media perfusion to cells in 3D cultures over time. We successfully generated HLC positive for hepatic markers such as ALB, CYP3A4 and CK18. AEC-derived HLC displayed early signs of hepatocyte phenotype, secreted albumin and urea, and expressed Phase-1 and -2 enzymes. The combination of liver-specific ECM and bioreactor provides a system able to aid differentiation into HLC, indicating that the innovative perfusion ECM-scaffold technology may support the functional improvement of multipotent and pluripotent stem cells, with important repercussions in the bioengineering of constructs for transplantation.

Keywords

Liver, extracellular matrix, decellularisation, bioreactor, stem cells, tissue engineering

Date received: 16 November 2023; accepted: 25 November 2023

[1]The Roger Williams Institute of Hepatology, Foundation for Liver Research, London, UK
[2]Faculty of Life Sciences and Medicine, King's College London, London, UK
[3]Department of Laboratory Medicine, Division of Pathology, Karolinska Institutet, Solna, Sweden
[4]Department of Medical and Molecular Genetics, School of Basic and Medical Bioscience, Faculty of Life Science and Medicine, King's College London, London, UK
[5]Centre for Biomolecular Spectroscopy, Randall Centre for Cell and Molecular Biophysics, Kings College London, London, UK
[6]Science for Life Laboratory, Division of Nanobiotechnology, Department of Protein Science, KTH Royal Institute of Technology, Solna, Sweden
[7]Department of Global Public Health, Karolinska Institutet, Solna, Sweden
[8]Department of Pathology and Cancer Diagnostics, Karolinska University Hospital, Huddinge, Sweden

*These authors have contributed equally to this work.

Corresponding author:
Luca Urbani, The Roger Williams Institute of Hepatology, 111 Coldharbour lane, London SE5 9NT, UK.
Email: luca.urbani@researchinliver.org.uk

Graphical abstract

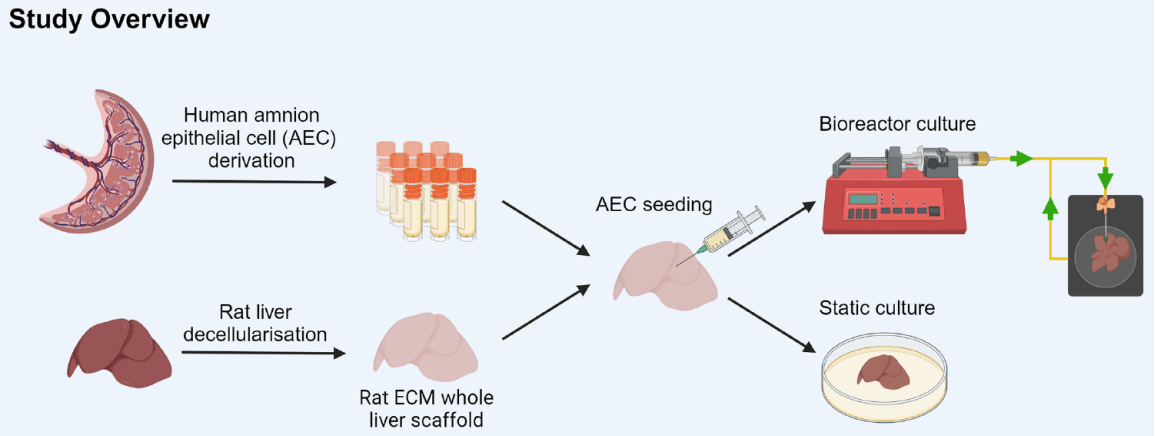

Background

More than 2 million deaths per year worldwide are attributed to complications arising from acute and chronic liver disease. Most of the patients die while waiting for a suitable organ for orthotopic liver transplantation, currently the only established curative treatment available for patients with terminal chronic liver disease and liver failure.[1–3] Nevertheless, liver transplantation has many drawbacks, including the cost and invasiveness of the surgery, scarcity of donors and lifelong need for immunosuppression with associated risks.[4] More than 150 patients have benefitted from an alternative cell-based therapy during the past 30 years: allogeneic hepatocyte transplantation has offered a correction to congenital disorders and temporary support to fulminant hepatitis to support over innate regenerative capacity.[5] However such alternative cell treatment is not free of limitations and equally suffers from a lack of donors and immunosuppression requirement.[6] Consequently, alternative solutions are needed to overcome the decrease in survival rate and increase in mortality attributed to liver disease.[7]

Transplantation of bioengineered liver grafts or extracorporeal devices with embedded functional human liver grafts can be promising approaches to support missing liver functions and provide secretive mediators. Preserving the crucial components and compartments of the organ, such as micro- and macro-vasculature, extracellular matrix (ECM) 3D architecture and biochemical properties, including the presence of active biomolecules, are key objectives to guarantee the organ's adequate functions while producing an engineered liver in vitro for transplantation.[4,8] The organ-specific ECM is a complex network of core proteins and tissue-specific molecules secreted by parenchymal cells, with specific effects on cell proliferation, differentiation and intralobular migration.[9] Decellularisation is a technique that allows for the removal of all organs cellular components while preserving intact ECM structure and composition.[10] Decellularised whole liver scaffolds retain the complex organ architecture intact, including venous and arteriosus vessels, but also potentially bile ducts and inter-hepatocyte trabeculae. Furthermore, several biochemical and biophysical properties of the native liver are largely preserved, with intact ECM and growth factors within, supporting stem cell differentiation into liver cells.[11–16]

Cells can only survive within a limited distance (up to ~1 mm) from a source of nutrients. Since decellularised organs are usually several millimetres thick, there are challenges associated with adequate nutrition supply and oxygen perfusion when used in ex vivo conditions, frequently resulting in non-functional areas or necrotic regions.[17] One of the major advantages of bio-engineering tissue equivalents is to recreate physiologically relevant culture conditions to accurately recreate the cellular microenvironment, and this is achievable also thanks to the use of fluidic systems, such as bioreactors. Bioreactors provide a constant nutrient supply while mimicking the natural cellular environment, enabling indirect monitoring of cellular behaviour in a non-invasive way.[18,19] There is a long history of bioreactor use in cartilage and bone engineering, showing that perfusion of culture medium at optimal flow rate can mimic the blood flow, as well as promote cell maturation and differentiation.[20]

We have previously designed and described a bioreactor allowing long-term perfusion culture of whole rat liver ECM scaffold.[12] In our previous work primary human hepatocytes were seeded in decellularised rat livers and cultured in a bioreactor is formed by a sterile chamber filled with liquid medium and connected to a programmable pump to ensure smooth perfusion of nutrients and oxygen through the cannulated vasculature of the decellularised liver scaffold. HepG2 cells as well as primary hepatocytes have proved the beneficial effects of bioreactor culture,

with improved hepatic gene expression (HNF4a, CYP1A2 and CDH1), as well as albumin and urea secretion, compared to hepatic cells cultured for long-term (up to 30 days) in static 2D condition. However, the use of immortalised cell lines or primary human hepatocytes has put significant roadblocks preventing the routine use of bioengineered liver constructs in toxicology studies or clinical use. Primary human hepatocytes have been proposed as the first-in-line choice for such studies, but the limited availability of these cells in addition to short-term survival and functional capacity in 2D or 3D conditions in vitro has encouraged researchers to identify new sources of cells for bioengineered liver constructs, as well as defining better condition to mimic the liver microenvironment for better restoration of liver functions.[21]

The ideal source of cells for the development of bioengineered liver constructs should be characterised by easy access, low cost for manufacturing and abundant amount of donor cells to seed in the bio-construct. In addition, such donor cells should support or provide secretive and metabolic hepatic activities. Pluripotent stem cells (such as iPSC and ES)-derived hepatocytes have shown limited maturation capacity, hampered by costs and ethical and genetic stability concerns. A further negative caveat is represented by the chronic inflammatory milieu in response to allograft, which favours the oncogenic transformation of transplanted cells. As detailed in a recent publication,[22] to efficiently generate mature and functional hepatocytes, undifferentiated stem cells need to be exposed to both inductive and repressive signals, to drive the cell through primitive steak, then definitive endoderm, progenitor, hepatoblast and finally mature hepatocyte (with relative difference in regards to the lobule localisation). Current ex vivo protocols involve hormonal and chemokines in very precise and articulated combinations. Such protocols have been largely described, including several variations and extensions, but essentially involve supplementation with OSM, ITS and HGF, and require approximately 3 weeks to reach mature hepatic potential. However, as abundantly described, a large part of the experimental approaches generates 'impure' and heterogenic populations containing a subset of (mature and functional) HLC. Mimicking developmental biology in an in vitro system has, and still does, required several revisions and refinements. In order to enhance and optimise such ex vivo commitment, a precise and tuned mapping of cells generated and undergone through all endodermal lineages (up to fetal hepatoblast or postnatal hepatocyte) has been recognised as critical. Finally, cell substrate and adhesion protein have also been depicted as critical and important in such regards. Somatic or perinatal stem cells, characterised by anti-inflammatory and pro-angiogenic features, have sparked enthusiasm for the generation of hepatocyte-like cells (HLC), with successful maturation limited to the epithelial stem cells paving the surface of the amnion membrane. Human amnion epithelial cells (AEC) derive from the inner cell mass of the blastocyst, before three germ layers are formed, suggesting as such cells may maintain memory for several, if not, all the somatic cells.[23] Once released by amnion membrane,[24] intact AEC have been previously seeded over liver-relevant ECM proteins (such as collagen or laminin isoforms) with limited effect on hepatic differentiation.[25] Additional experimental attempts revealed that 3D strategies, such as inclusion into Matrigel substrate, only partially support AEC differentiation into hepatic cells.[25] Conversely, when human AECs were implanted into murine liver parenchyma, their maturation into fully functional liver cells in vivo was sufficient to rescue and correct animals with liver diseases.[26] Furthermore, transplanted cells displayed metabolic and synthetic hepato-specific activities.[27,28] This supports the hypothesis that an efficient and functional improvement of AEC along a hepatic lineage can be achieved only when cells are cultured on a liver-specific ECM. We hypothesised that a more physiological system, such as the one offered by perfused decellularised liver scaffolds, may offer support to overcome such incomplete differentiation into functional HLC.[29]

In this study, we investigated the possibility of generating functional and mature liver constructs by culturing AEC in decellularised whole rat liver scaffolds with the support of a bioreactor, designed to support the functional differentiation of human AEC into hepatocytes, in 3D conditions. The acquired hepatic functions were assessed longitudinally throughout the culture, for all the functional and cellular characteristics. We show that the presence of liver ECM-scaffolds supported the differentiation of AEC into functional HLC and that the perfusion of media improved cell distribution and hepato-specific activities compared to static culture conditions. Although similar technological approaches have been applied to other stem cell populations, this is the first proof of principle study that combines perfusion bioreactor, decellularised liver-specific ECM and AEC. The technology here presented can serve as a paradigm for hepatic maturation in a 3D model of the liver composed of natural ECM and can help to investigate the role of ECM-specific proteins in cell differentiation and functionality.

Materials and methods

Liver harvesting and decellularisation

All surgical procedures done in this study and the animal husbandry are in accordance with the recommendations in the Animal (Scientific Procedures) Act 1986 and the local Ethics Committee. Livers were harvested from wild type rats (~300 g) which were euthanised by CO_2 inhalation. Liver isolation and canulation of the vena cava for perfusion-decellularisation was performed as previously

described.[11] Briefly, the abdomen of the rats was sterilised with 70% ethanol (EtOH; VWR, Radnor, Pennsylvania, USA) and the abdominal-pelvic cavity was exposed. The inferior vena cava (IVC) and portal vein (PV) of the liver were identified. Firstly, The IVC was tied with silk sutures (FST, Cambridge, UK) while the PV was cannulated with a 24G cannula (Terumo, Fisher Scientific, Loughborough, UK). The liver was then released from the surrounding tissue, and perfused with sterile phosphate buffer saline (PBS; Sigma, Gillingham, Dorset, UK) with 1 U/mL heparin (Sigma) to check for leakage and remove the excess blood, followed by the perfusion of 1mM ethylenediaminetetraacetic acid (EDTA; Sigma) to prevent blood clots in the vessels.

Decellularisation was started directly after liver harvest by perfusion of a series of solutions through the vasculature network. A variable speed roller pump (iPumps, Pamington, UK) was connected to the cannulated PV by silicon tubes (Saint-Gobain Performance Plastics, Courbevoie, France). To block the entrance of any air into the system a microfluidic bubble trap (Kinesis®, Cole-Parmer®, Eaton Socon, UK) was used. All tubes were also primed with UV radiated ultrapure (MilliQ) water to eliminate any air before the start of the process. The decellularisation process was initiated by perfusion of MilliQ water for 18 h at a 4.5 mL/min flow rate, followed by 4% sodium deoxycholate (SDC; Sigma) for 5 h at 6.5 mL/min at room temperature. PBS and then 25 mg/L DNase-l (Sigma) in saline solution (0.15 M NaCl, 10 mM $CaCl_2$, Sigma) were perfused through the vasculature for 1 and 3 h, respectively, at 6.5 mL/min, both solutions were warmed and maintained at 37°C. The scaffolds were perfused by warm PBS at 6.5 mL/min for 1 h, and then 25°C PBS at 1 mL/min overnight. The scaffolds were then sterilised by 90 min perfusion of 0.1% Paracetic Acid (PAA; Sigma) and 4% Ethanol in MilliQ water, followed by 90 min perfusion storage solution (composed of 1% Penicillin-Streptomycin (Gibco, ThermoFisher Scientific, Waltham, Massachusetts, USA)) with 50 ng/mL Primocin (InvivoGen, Toulouse, France) in PBS. Scaffolds were finally gamma-irradiated and stored at 4°C in the storage solution.

For vascular perfusion assessment, the decellularised rat ECM whole liver vasculature was flushed once with PBS then gradually perfused via the PV with 1% trypan blue in PBS using a programmable syringe pump at 1 mL/min for 3 min. Perfusion was filmed and still shots were taken every 30 s for up to 3 min.

DNA quantification

To determine decellularisation efficiency, total DNA of fresh rat liver and decellularised rat livers was isolated using DNeasy Blood and Tissue kit (Qiagen, UK) as per the manufacturer's instructions. Yield and purity were measured spectrophotometrically at 260 and 280 nm using a Nanodrop (Thermo Scientific, USA).

The DNA concentration was also analysed to estimate the total amount of DNA in rat ECM whole liver scaffolds seeded with AEC, as a proxy of the number of cells present at day 15 and at day 30 of culture in static or in the bioreactor. The total amount of DNA was calculated by dividing the amount of DNA extracted by the weight of the tissue sample it was extracted from and then multiplying for the weight of the whole liver scaffold.

Elastin quantification

Elastin content (including soluble tropoelastins, lathyrogenic elastins and κ-elastin) was quantified using a commercial assay kit (Biocolor, UK) as per manufacturer's instructions. Liver samples were homogenised and solubilised in 0.25 M oxalic acid, then incubated at 95°C. 5,10,15,20-tetraphenyl-21H,23H-porphine tetrasulfonate (TPPS) dye, which binds soluble elastin, was added to the sample extracts. Excess dye was removed by centrifugation. Elastin-dye complex was separated with the addition of a dye dissociation reagent, and the resulting solutions were measured spectrophotometrically at 555 nm. Elastin quantity was calculated from a standard curve plotted with known elastin concentrations.

Human AEC isolation

The human AEC isolation was performed as previously described.[30–32] Briefly, the amnion membrane was removed from the inner layer of the placenta from full-term healthy pregnancies, and washed extensively to remove blood. The amnion membrane was immersed in TrypLE 10x (Gibco) for 30 min at 37°C to release mainly AEC from the amnion membrane. The released AEC were collected and washed by serial centrifugation and filtered through a 100 μm cell strainer to remove undigested tissues or large clamps. Cell viability and yield were determined by the Trypan Blue exclusion and cells immediately exposed to cryopreservation procedure.

Cryopreservation procedure

Freshly isolated AEC were resuspended in DMSO-supplemented solution and cryopreserved as previously described.[33] The cells were stored and delivered in the vapour phase of a liquid nitrogen storage tank. On the day of the experiment, the cells were removed from the liquid nitrogen tank and rapidly thawed at 37°C. Cells and DMSO-supplemented solution were immediately diluted and centrifuged at 250*g* for 5 min. The cell pellet was resuspended in expansion medium for seeding.

Human AEC seeding into rat ECM whole liver scaffolds

Cryopreserved AEC were seeded in the rat ECM whole liver scaffolds by direct injection to the portal vein.

Seeding was performed via perfusion through a canula using a programmable syringe pump (iPumps) at an infusion rate of 3 mL/min, for a total volume of 12 mL of cell suspension per seeding of AEC 'expansion medium' (please refer to Methods section 'AEC 3D culture and hepatic differentiation and Supplemental Table 1 for details). On average, 43.8 ± 2.62 million viable cells were seeded into each rat ECM whole liver (10 scaffolds were used in total). This number reflects the seeding density previously used by our group in a similar study with primary human hepatocytes and rat ECM whole liver scaffolds.[12] Three consecutive infusions required approximately 66 min, with 10 min incubation steps between infusions. After the third infusion, non-attaching AEC were collected and centrifuged at 250*g*, and counted to indirectly assess cell retention into the scaffold. After perfusion-seeding, the rat ECM whole liver scaffolds were incubated in static condition for 48 h, prior to initiating the perfusion culture in the bioreactor or continuing in static condition as control. This static incubation step was performed in order to allow the cells to adhere to the ECM of the liver scaffold, prior to commencing the perfusion of media.

AEC 3D culture and hepatic differentiation

Human AECs were cultured in the rat ECM whole liver scaffolds with or without a first step using 'expansion medium' (modified from Morandi et al.[34]) composed of: Iscove's Modified Dulbecco's Medium (IMEM 1X, Gibco), supplemented with 5% Stemulate (Biolife solutions), 1% Sodium Pyruvate 100 mM (Gibco), 1% MEM Non-essential Amino Acid Solution (100x, Sigma), 0.05% β-Mercaptoethanol in DPBS (1 M, Sigma), 1% Penicillin/Streptomycin (with 10,000 units penicillin and 10 mg streptomycin/mL, Gibco) and 1% L-Glutamine (200 mM, 100X, Gibco), 50 µg/mL Epidermal growth factor (EGF, 200 µg/mL, Peprotech, London, UK), 0.05% Primocin solution (50 mg/mL, InvivoGen). Upon seeding of the scaffold, AEC were expanded in 3D in expansion medium for 10–12 days. After the expansion period, cells were exposed to the 'hepatocyte differentiation medium' composed of Dulbecco's Modified Eagle Medium (DMEM 1X, Gibco) and Williams' Medium E (1X, Gibco) in a ratio of 1:1, supplemented with 0.5% MEM Non-essential Amino Acid Solution (100x, Sigma), 1% Dimethyl Sulfoxide (DMSO; Hybri-Max™, Sigma), 1% L-Glutamine (200 mM, 100X, Gibco), 1% Penicillin-Streptomycin (with 10,000 units penicillin and 10 mg streptomycin/mL, Gibco), 1% HEPES solution (1 M, Sigma), 0.5 µM Dexamethasone (10 mM, Sigma), 1% Insulin-Transferrin-Selenium (100X, Gibco), 0.1 µM Hydrocortisone (1 mM, Sigma), 10 ng/ml Hepatocyte growth factor (HGF; 100 µg/ml, Peprotech), 25 µM Gentamycin solution (50 mg/ml, Sigma). Expansion and differentiation media were replaced every three days of perfusion culture in the bioreactor by withdrawing and adding media into the fluidic system via a three-way connector (Cole-Parmer®, Eaton Socon, UK) using a disposable syringe, avoiding bubble formation. Hepatic differentiation required 20–30 days, and 25 µM rifampicin (0.1 mM, Sigma-Aldrich) was added to the culture medium within approximately 10 days and refreshed until the end of the hepatogenic period to promote early differentiation. At each feeding, approximately 3ml of circulating media was collected and stored at −80°C for analyses. Media compositions are summarised in Supplementary Table 1.

Bioreactor settings

The bioreactor system utilised here was manufactured and assembled as previously described in Sassi et al.[12] Briefly, the bioreactor is composed by a chamber with a keyhole shape: a circular part for housing the organ and a rectangular element for housing cannulas and tubes. The bioreactor was connected to a programmable syringe pump (World Precision Instruments R) to allow the semi-continuous flow of medium. To avoid air bubbles, a bubble trap (Kinesis Scientific) linked to a vacuum assistance was implemented. The chamber was manufactured using Computer Numerical Control machine, for which the settings, as well as a picture of the set-up, are explained in the original manuscript.[12] For cell seeding, cells were delivered into the scaffold through the portal vein at 4 mL/min. During culture, the pump was set to 1 mL/min of semi-continuous flow.

Histological analysis and immunostaining

Sample fixation and embedding. Fresh rat livers, decellularised rat ECM whole liver scaffolds, and seeded scaffolds were analysed by histology. Tissue segments were fixed in 4% paraformaldehyde (PFA; Sigma) for ~2 h at 4°C, briefly washed with PBS, and cryoprotected by immersing in 30% sucrose (Sigma) solution in PBS overnight. Tissue segments were then blotted in absorbent paper to remove the excess of sucrose (Sigma), embedded in OCT (VWR) and placed on dry ice for 10–20 minutes to set. 6–10 µm thick tissue sections were generated using a cryostat (Bright Instruments, Huntingdon, UK), and positioned on glass slides (Epredia™, Fisher Scientific, Leicestershire, UK), which were used in later analysis.

Haematoxylin and Eosin (H&E) staining. Prepared slides containing OCT-embedded tissue sections were air dried and the excess OCT was washed by placing the slides in PBS for 5 min in a Coplin jar, followed by a brief wash with distilled water. Slides were then placed in haematoxylin (Richard Allan Scientific™, Epredia™) for 4 min and rinsed under running tap water for 2 min. Slides were briefly differentiated in 70% ethanol + 1% HCl (Acid

Alcohol), then rinsed well with running tap water, and consequentially incubated in eosin (Eosin Y Solution, Sigma) for 1 min. Slides were washed with running tap water again before being placed in three increasing concentrations of ethanol to induce sample dehydration: 70% ethanol for 10 s, 90% ethanol for 30 s and 100% ethanol for 30 s. The slides were then placed in Histo-Clear (National Diagnostic, Atlanta, Georgia, USA) for 5 min. Finally, Neo-Mount™ (Sigma) was added on the coverslips which were used to mount the slides. Slides were dried overnight prior to imaging.

Picrosirius Red. Picrosirius Red staining for collagen type I and II was carried out using Picrosirius Red Stain Kit (Polysciences, USA) as per manufacturer's instructions. Briefly, cryopreserved tissue sections were washed with PBS and then fixed in 10% Formalin for 10 min at room temperature. After fixation, the slides were rinsed in copious amounts of ddH2O and stained with Picrosirius Red (solution B) for 30 min (fresh tissue) or 5 min (decellularised tissue). Sections were dipped twice in HCl (solution C) and then rinsed in ddH2O. Finally, sections were dehydrated in 100%, 90% then 70% ethanol and left to dry before mounting and imaging.

Immunofluorescent staining. Slides prepared with OCT-embedded tissue sections were first washed with PBS to dissolve the OCT.

Slides staining for CYP3A4 and Ki67 markers underwent antigen retrieval. This was performed by immersing slides in a pre-heated (900 W microwave, 8min) solution of 0.1 M citrate buffer (pH6) for 15 min. All slides were then blocked for unspecific binding by incubating with a blocking solution containing 1% bovine serum albumin (BSA; Sigma) and 0.1% Triton-X1000 (PBS-T; Sigma) in PBS (30 min incubation at room temperature). Afterwards, slides were incubated with primary antibody (specified in Supplemental Table 2) diluted in PBS-T (0.01%) + 1% BSA diluent solution, and incubated overnight at 4°C. Slides were then washed three times with PBS with 5 min incubation for each wash. Subsequentially, appropriate secondary antibodies were added after dilution (1:500) in the same diluent solution as the primary antibody, together with DAPI (1:1000, ThermoFisher Scientific) to identify the nuclei. Slides were incubated at room temperature for 45 min. They were then washed with PBS three times. An additional incubation of 10 minutes at room temperature with 0.1% Sudan Black solution (Sigma; made in 70% ethanol) was done to reduce the background, followed by a wash with running tap water and a rinse with distilled water to remove the excess Sudan Black. Finally, few drops of anti-fade mounting media (Abcam, Cambridge, UK) were added to each slide and coverslips (cover glasses, 1.5 thickness, VWR) were placed on them. Slides were left to dry and stored at 4°C prior to imaging.

Imaging and analysis. Immunofluorescence and H&E imaging were performed with Olympus BX43 fluorescence microscope (Olympus, Hamburg, Germany) using the CellSens software. Image analysis for fluorescence intensity was performed using Fiji-ImageJ software. Immunofluorescent staining of seeded scaffolds was analysed using digital pathology software QuPath (version 0.4.4). Images from six random regions of interest were combined into one training image. Then, the built-in cell detection thresholder from QuPath was set to count cells based on the DAPI staining in six regions of interest per biological replicate ($n = 3$). Following cell detection, an object classifier using the Random Forest algorithm was trained by the experimenter to identify and quantify positive cells for markers CK18, CK19 and Ki67.

EROD assay

The conversion of the nonfluorescent substrate 7-ethoxyresorufin, to the fluorescent product resorufin, is mediated by a CYP1A activity, and we used this to assess CYP1A1 and 1A2 activities in cells as previously described.[21] This phase 1 assay (named EROD) is based on the increase in fluorescence of resorufin, when the 7-ethoxy terminal is removed through CYP1A1/2 enzymes within cells. Salicylamide addition to the initial reaction inhibited the conjugation of the final product, resorufin, allowing quantification of metabolic reaction.

Before performing the assays, the following reagents were dissolved in DMSO: 20 mM 7-ethoxyresorufin (Tocris, Biotechne, Minneapolis, Minnesota, USA); 1.5 M salicylamide (Merk Millipore, Darmstadt, Germany). All stock solutions were kept in the dark at −20°C until use. A few minutes before performing the assay, the compounds were thawed and diluted 1000-fold into William's medium (ThermoFisher Scientific). Upon dilution, 7 mL of William's medium supplemented with 7-ethoxyresorufin and salicylamide were perfused in the whole rat liver scaffolds (removed from the bioreactor or static culture plate and placed in a new 10 mL petri dish) using a syringe connected to the cannula, and then the scaffolds were incubated at 37°C for 30 min in the dark. After incubation, 80 µL of the perfused solution were transferred in a 96-well black plate (in triplicate) and read using a fluorescence spectrophotometer with an excitation wavelength of 535 nm and an emission wavelength of 581 nm, with a sensitivity of 35 nm (BMG LabTech, Ortenberg, Germany). The assay was performed at every feeding (every 3 days) in the differentiation culture conditions. The linear range between 0.5 and 50 ng/mL of resorufin (Merck Millipore) was determined after establishing a standard curve that was used to extrapolate resorufin concentration in the samples. Furthermore, resorufin concentration in the medium was also reported after normalisation over the total amount

of DNA extrapolated for each scaffold collected at day 15 and day 30 of the culture.

Mycoplasma test

The commercial detection kit MycoProbe (R&D Systems, Biotechne, Minneapolis, Minnesota, USA) was used to test the mycoplasma contamination periodically, following the manufacturer's instructions. O.D. values generated from the media samples were then compared to the positive and negative controls with determined O.D. values.

Albumin and urea ELISA

To test hepatic functions of seeded AEC, aliquots of media were collected every 3 days of culture from the bioreactor and static controls. The concentrations of albumin and urea secreted by AEC in the culture medium were measured using enzyme-linked immunosorbent assays (ELISA): Human Albumin Assay Kit (E88-129, Bethyl Laboratories, FORTIS Life Sciences, Waltham, Massachusetts, USA); Urea Assay Kit (ab83362 Abcam, Cambridge, UK), following manufacturer's instructions. The concentration (ng/mL) for each sample was calculated based on the generated four-parameter fit standard curve using the Microsoft Excel software. Albumin concentration was calculated as total albumin amount in the supernatant considering the total volume of culture media, and also reported after normalisation over the total amount of DNA extrapolated for each scaffold collected at day 15 and day 30 of culture. Urea concentration is reported normalised over the total amount of DNA extrapolated for each scaffold collected at day 15 and day 30 of culture.

Nuclear magnetic resonance spectroscopy (NMR)

Media samples from bioreactor and static cultures during expansion and differentiation phases were analysed by NMR spectroscopy at the KCL Guy's NMR facility. All study samples showed confounding NMR peaks from DMSO (2.75–2.72 ppm), ethanol (3.69–3.63 ppm and 1.210–1.165 ppm) and residual water (4.86–4.72 ppm). These NMR regions were masked from ongoing analyses. Wiley KnowItAll v17.0 data analysis program was used for principal component analysis (PCA). MetaboAnalyst v5.0 was used for both PCA and Partial Least Squares Discriminant Analysis (PLS-DA).[35] Excluded regions for NMR analysis: >10.0 ppm; 4.90–4.70 ppm; 3.69–3.63 ppm; 2.75–2.72 ppm; 1.21–1.165 ppm; <0.01 ppm. The added TSP reference (0.01−(−0.01) ppm) was included to check stability and reproducibility of NMR sample preparation and NMR data acquisition. The NMR spectrometer was considered to be sufficiently stable that signal intensities were reported in five specific manually adjusted NMR regions: glucose doublet (5.26–5.22 ppm), alanine doublet (1.495–1.465 ppm) lactate and threonine overlapping doublet region (1.35–1.31 ppm) ADP, and valine doublet (1.06–1.03 ppm).

For the analyses, data points from bioreactor and static cultures from expansion (day 10) and differentiation (day 15, 24 and 30) were considered ($n=4$ each). Principal Component Analysis (PCA) [mean-centred, normalised] using Wiley KnowItall and MetaboAnalyst and Partial Least Squares Discriminant Analysis (PLS-DA) with Variable Importance in Projection plots (VIP) from KnowItAll were used.

RNA extraction and RT-qPCR

At the end of the culture experiments in differentiation medium (3D static and bioreactor cultures), total RNA was extracted by mechanical disruption of rat ECM whole liver scaffold-containing cells and cells' lysis in TRIzol reagent (Life Technologies) followed by Pure Link RNA Mini Kit (Life Technologies), according to manufacturer instructions. Adult hepatocyte total RNA was extracted after cell lysis in TRIzol, followed by Pure Link RNA Mini Kit, according to manufacturer instructions. cDNA was synthesised using the High Capacity Reverse Transcriptase Kit (Life Technologies) according to manufacturer's protocol. Following cDNA synthesis, RT-qPCR was performed using TaqMan Universal PCR Master Mix (Applied Biosystems) and quantitative expression analysis was performed with TaqMan gene expression assays using a StepOnePlus system (Applied Biosystems, Life Technologies). The thermal cycle started with incubation for 2 min at 50°C, followed by 10 min at 95°C and finally 40 cycles of 15 s at 95°C and 1 min at 60°C. The cycle threshold was set to 0.082963 in all experiments. This threshold was well within the linear range of all amplification curves. Reactions were run in duplicate or triplicate, with GAPDH mRNA as an endogenous control in all experiments. Calculation of relative levels of expression was done according to the comparative Ct-method as follows: 2(−DCt), where DCt = Ct gene of interest − Ct internal control GAPDH. Ct values for the gene of interest 35 or higher were excluded, as considered unreliable.

Flow cytometric analyses

Evaluation of plasma membrane adhesion molecule expression was performed in seven different cryopreserved AEC batches, using fluorochrome-conjugated monoclonal antibodies (as listed in Supplemental Table 2). Briefly, cells were exposed to antibodies directed against CD18 (Becton Dickinson; clone 6.7); CD29 (Becton Dickinson; clone 38047); CD49a (BioLegend; clone TS2/7); CD49c (BioLegend; clone ASC-1); CD49d (Becton Dickinson; clone 9F10); CD49e (Becton

Dickinson; clone IIA1); CD49f (US Biologic; clone 7H164); CD51 (BioLegend; clone NKI-M9); CD61 (Becton Dickinson; clone VI-PL2); CD104 (BioLegend; clone 58XB4); beta5 integrin subunit (BioLegend; clone AST-3T); beta7 integrin subunit (BioLegend; FIB504). FITC-, PE- or APC-conjugated irrelevant isotype-matched monoclonal antibodies were purchased from Becton Dickinson or BioLegend. Cells were analysed with FACSCanto (Becton Dickinson) and data was shown as a percentage of positive cells.

Statistical analysis

Data were initially calculated and processed using the Microsoft excel software and presented by mean ± standard deviation (SD). Different statistical analyses were done on different groups of data using GradPad Prism (version 5.03, GraphPad Software Inc.), *t*-test was performed to compare two groups, while two-way ANOVA was done to perform multiple comparisons between different groups of data. p Value <0.05 was chosen as the minimum level of significance.

Results

The experimental design and timeline of the 3D culture of cryopreserved AEC in decellularised rat ECM whole liver scaffolds are shown in Figure 1(a). Rat ECM whole liver scaffolds were assessed for complete removal of cellular components (decellularisation efficiency) and preservation of hepatic 3D architecture (Figure 1(b)–(e)). A full characterisation of the rat ECM whole liver scaffold post-decellularisation was previously described by our group,[11] in particular the preservation of collagen content. We confirmed the decellularisation efficiency by assessing the optical purity of the scaffolds (Figure 1(b)), vascular patency, essential for cellular perfusion-repopulation (Figure 1(c)) and absence of the cellular compartment with H&E staining (Figure 1(d)) and DNA quantification (Figure 1(e)). In addition, as relevant to the vasculature structure, we determined that the decellularisation process maintained the overall structure and architecture of the liver ECM scaffold, including the collagen network (picrosirius red staining, Figure 1(d)) and the total elastin content in the ECM after decellularisation (Figure 1(e)).

Seven different human donor derived AEC were infused in distinct rat ECM whole liver scaffolds. Both cell viability post-cryogenic storage and distribution and identity of the cell suspension were confirmed: AEC viability after thawing ranged between 80% and 95%; 99% percentage of cells were positive for E-cadherin and epithelial integrin subunit CD49f, in addition to epithelial cell adhesion molecule (EpCAM/CD326) (Table 1). In addition to AEC identity markers, we commonly excluded possible contaminants for mesenchymal cells or human leukocytes in every AEC batches (<2% cells positive for CD105 and CD90, and <0.2% CD45 positive cells, respectively).[30]

To evaluate potential capacity to adhere to liver ECM scaffold, we profiled a complete set of ECM-adhesion proteins on cryopreserved AEC: we measured constitutive presence of beta 1 and 4 integrin subunits and alpha 6 and V molecules, known for being the cell bridge towards ECM molecules such as laminins, collagen, fibronectin and osteopontin (Table 1).

Each rat ECM whole liver scaffold was seeded with 43.8 ± 2.62 million cells. After seeding, scaffolds were gradually repopulated and showed a different appearance going from a transparent scaffold to a more white-yellow colour, indicating the presence of cells in the matrix (Figure 1(f)). Cell retention after seeding was calculated at 91%. Cell-seeded scaffolds were maintained either in static condition, immersed in the culture medium in a Petri dish, or in the bioreactor, in which the medium was perfused in the custom-made chamber harbouring the scaffold (Figure 1(g)).[12] The perfusion of medium in the bioreactor was initiated 2 days after seeding, and for the first 10 days of culture, cells were exposed to expansion medium, and switched into differentiation medium until the end of the experiment (20 to 30 days of differentiation). The cultures in bioreactor preserved sterility and were mycoplasma-free throughout the culture period (O.D. values <0.5, Supplemental Table 3).

AEC-seeded scaffolds cultured for up to 40 days in both static and bioreactor conditions showed comparable homogeneous cell distribution with large areas repopulated by cells and similar total DNA extrapolated for each scaffold collected at day 15 and day 30 of differentiation (Figure 2(a)–(c)). We used keratin 18 and 19 to identify the presence of AEC-derived hepatic parenchymal cells (hepatocytes and cholangiocytes respectively).[36] Immunofluorescence analysis showed AEC expressed both keratin 18 (CK18) and keratin 19 (CK19) at a higher level when cultured in bioreactor conditions compared to static conditions (Figure 2(d)–(f); Supplemental Figure 2), although these trends were not significant. We found that the expansion step after seeding was not critical to enhancing engraftment and distribution of AEC within different liver lobes, neither in static nor bioreactor conditions, as the presence of proliferating $Ki67^+$ cells was not different between the two culture conditions (Figure 2(d)) (Ki67-positve cells were below 1% in both conditions – data not shown). Human AEC have been largely described as negative for mesenchymal or endodermal markers (such as CD90 and SOX9) upon isolation,[37] and such low expression was confirmed upon hepatic differentiation (Supplemental Figure 1).

The expression of hepatocyte functional markers such as albumin, E-Cadherin, CYP3A4 and HNF4α supported the evidence of AEC differentiation into HLCs in 3D

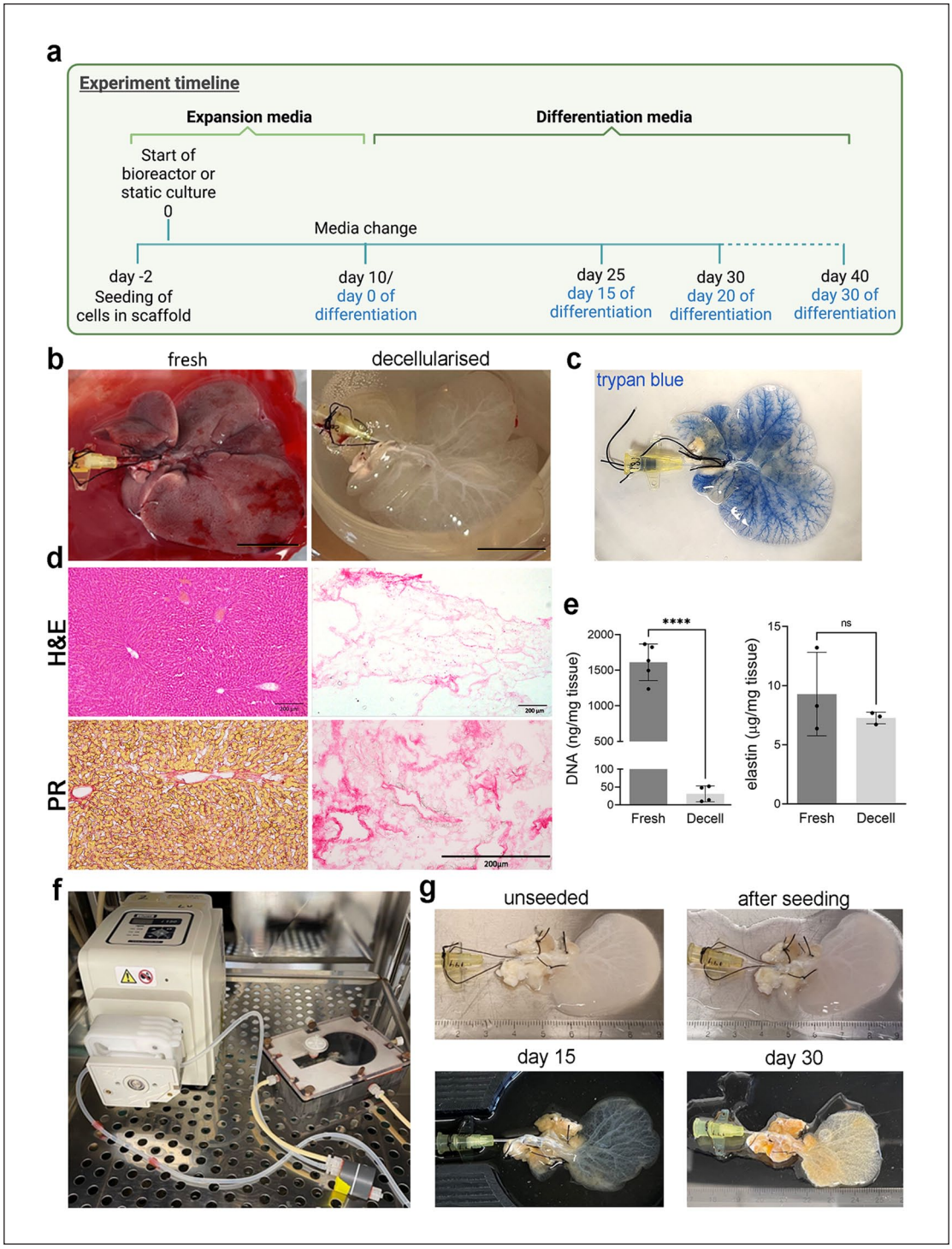

Figure 1. Experiment timeline and overview, scaffold characterisation and seeding: (a) experiment timeline for seeding and differentiation of AEC, (b) representative images of fresh and decellularised rat liver showing the scaffold becoming completely transparent after the decellularisation procedure (scale bar: 2 cm), (c) vasculature patency assessment using perfusion of trypan blue solution via the portal vein, (d) representative Haematoxylin and Eosin (H&E) and picrosirius red (PR) staining of fresh and decellularised rat liver scaffolds showing absence of nuclei and preservation of the ECM architecture and overall collagen network post-decellularisation (scale bar: 200 µm), (e) quantification of elastin and DNA content in fresh and decellularised livers ($n = 3–5$; mean ± SD; *t*-test), (f) representative image of the bioreactor set-up (connected to a peristaltic pump) in the incubator, and (g) representative images of AECseeded scaffold at different time points showing the presence of cells at the end of the culture (darker yellow).

Table 1. FACs analysis of ECM-adhesion molecules expressed by AEC.

Cell-ECM adhesion molecule	Percentage (range)	Function
Integrin β1 subunit (CD29)	99–100	Adhesion molecule for fibronectin, collagen type I–IV
Integrin β2 subunit (CD18)	0.01–0.02	Adhesion molecule involved in T cell activation/extravasation
Integrin β3 subunit (CD61)	0.02–0.05	GP3a, adhesion molecule for fibrinogen
Integrin β4 subunit (CD104)	94–99	Adhesion molecule for laminin
Integrin β5 subunit	0.3–0.9	Heterodimers with αV, receptor for fibronectin
Integrin β7 subunit	0	Heterodimers with α4, responsible for efficient trafficking and retention of lymphocytes
Integrin α1 subunit (CD49a)	0.04–0.08	Adhesion molecule for collagen IV
Integrin α3 subunit (CD49c)	65–74	Adhesion molecule for collagen, laminin, fibronectin and thrombospondin
Integrin α4 subunit (CD49d)	0.01–0.03	Adhesion molecule for fibronectin, and involved in intercellular interaction with leucocytes
Integrin α5 subunit (CD49e)	20–63	Adhesion molecule for fibronectin
Integrin α6 subunit (CD49f)	98–99.5	Heterodimers with β1 or β4, adhesion molecule for laminin/kalinin
Integrin αV subunit (CD51)	98–99.5	Heterodimers with β1, β3, β5, β6 or β8, adhesion molecule for vitronectin (α chain), osteopontin, fibrinogen, laminin

culture conditions in liver ECMs. Histological analyses showed an overall stronger expression of HLC markers in bioreactor scaffolds than in static conditions (Figure 2(g)–(j)), although the quantification of CYP3A4 expression showed comparable levels in the two culture conditions (Figure 2(i)). In particular, CK18-positive cells were found co-expressing HNF4α in bioreactor cultures (Figure 2(j)), and AEC-derived HLCs exhibited lower expression levels of alpha-feto protein (AFP) in bioreactor-cultured scaffolds than in static conditions (Figure 2(g)). The epithelial marker EpCAM, constitutively expressed by naïve AEC as well as bile duct cells,[30] was lost during improvement of functional differentiation into HLC (Figure 2(h)).

Stem cell-derived HLCs have been described as lacking hepatic maturity, resembling more the functions of fetal hepatocytes, rather than adult cells.[38,39] Specifically, such incomplete maturation has been described for AEC limitedly in in vitro culture, but greatly improved when liver ECM was supplemented to AEC.[25] We confirmed the differentiation status of AEC-derived HLC by gene expression analyses and tested the results in comparison with adult human liver tissues (Supplemental Table 4). The first step towards hepatoblast formation is the increased secretion of AFP, followed by a progressive loss in such serological markers in favour of postnatal albumin and early-stage CYPs (1A1 and 3A7 enzymes) expression. We detected a progressive increase in the expression for both early-stage CYPs, with a higher expression in bioreactor cultures compared to static conditions. Interestingly, we observed a higher level of expression for *CYP1A2* in static conditions with respect to the perfusion bioreactor, indicating partial maturation and different expression dynamics of CYPs during differentiation in presence of interstitial flow (Figure 3(c)). Although the gene expression levels are considerably lower than the ones in adult liver, perfusion in bioreactor frequently resulted in a higher expression of several hepatic genes, such as *A1AT*, *UGT1A1* and *HNF4α*, indicating that partial differentiation of AEC cells to HLC is aided by the perfusion culture, similarly to the results obtained from protein expression analysis in Figure 2 (Figure 3(d)–(f)) and Supplemental Table 4).

Hepatic function was assessed longitudinally in both culture conditions. Albumin secretion in the culture media was significantly higher in the bioreactor culture in comparison with static conditions (Figure 4(a)), with a decrease in production rate (slope) after 21 days. This decrease in cell function after 21 days was confirmed by the calculation of albumin normalised on an indirect measurement of cell density (total DNA extrapolated for each scaffold), which showed a relative decrease in albumin secretion at day 30 of culture (Figure 4(b)). Nevertheless, bioreactor cultured scaffolds still produced higher amounts of albumin in respect to static conditions. Similarly, urea concentration was also significantly higher in the circulating culture media collected from the bioreactor circuit in comparison to media collected from static cultures at different time points during differentiation, although with a relative decrease at day 30 of differentiation in both culture conditions (Figure 4(c)). CYP1A activity was measured every 3 days throughout the differentiation period by quantification of resorufin in the media upon its conversion from non-fluorescent substrate 7-ethoxyresorufin (EROD assay) (Figure 4(d) and (e)). Resorufin was detectable in both culture conditions from day 3 of differentiation and its concentration increased during the culture. A stronger 7-ethoxyresorufin conversion by HLC was detected in constructs cultured in bioreactor conditions compared to static conditions, with peak function between 24 and 27 days in differentiation media, similarly to what detected with albumin and urea quantification. The metabolic profile of cells cultured in ECM-scaffolds in expansion and differentiation media determined

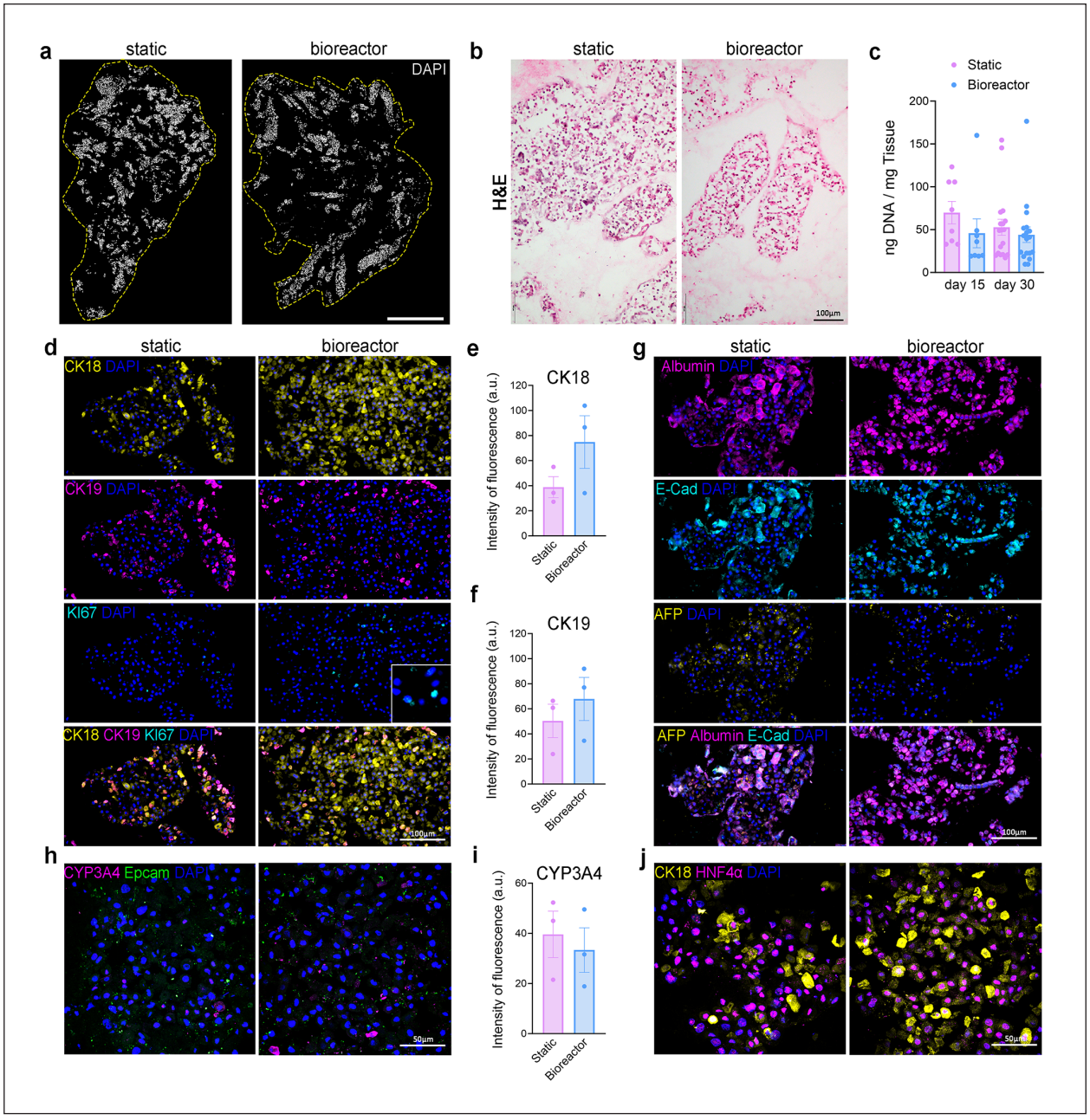

Figure 2. Distribution and phenotype analysis of AEC cultured in liver ECM scaffolds: (a) representative maps of cells stained with DAPI in scaffolds cultured in static or bioreactor conditions showing repopulated areas (scale bar 100 μm), (b) H&E staining showing AEC clusters in repopulated areas (scale bar 100 μm), (c) DNA concentration in cultured scaffolds recovered after 15 and 30 days in differentiation media (mean ± SD; *t*-test), (d, g, h, j) immunofluorescence analysis of AEC seeded in ECM scaffolds and cultured in static or bioreactor conditions (scale bar (d and g): 100 μm, (h and j): 50 μm), and (e, f, i) quantification (via fluorescence intensity) of protein expression for CK178, CK19 and CYP3A4 ($n = 3$ biological replicates; mean ± SD; *t*-test).

with NMR, showed slightly higher consumption of relative amount of glucose by cells cultured in the bioreactor during expansion phase, while other metabolites did not show significant changes between conditions (Figure 4(f)). When cultured in differentiation media, cells increased the relative amount acetate released into the media, both in static and bioreactor conditions. Cells exposed to differentiation media in static condition showed continuous production of glucose, threonine and valine. HLC metabolite profile in bioreactor culture condition was different across time points, with peak release of glucose, alanine, threonine and valine at day 24 of culture (Figure 4(f)).

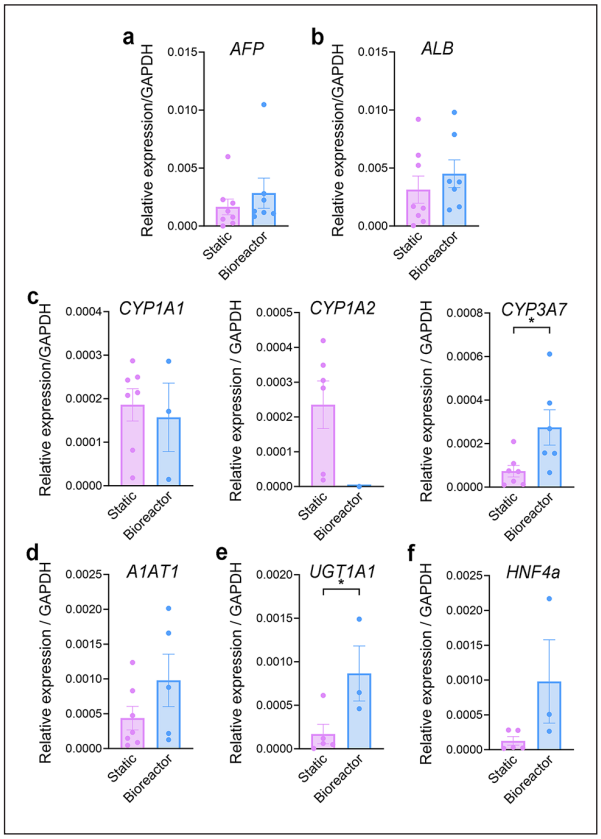

Figure 3. Hepatocyte functional gene expression analysis. qPCR analysis of hepatoblast and mature hepatocyte gene (AFP, ALB, A1AT1, UGT1A1, HNF4α) and CYPs enzyme gene (CYP1A1, CYP1A2, CYP3A7) expression in AEC cultured in rat ECM liver scaffolds. RNA was extracted from rat ECM whole liver scaffold-containing cells at the end of the 3D culture period (30 days in differentiation medium) in static or bioreactor conditions ($n = 3–8$). Mean ± standard deviation. *$p < 0.05$, *t*-test.

Discussion

Organ and tissue bio-engineering is considered one of the most promising alternatives to recreate the microstructure of healthy liver and support the innate capacity of the liver to regenerate. Furthermore, the possibility to maintain major hepatic functions and offer an accurate and human-relevant drug screening platform largely benefit preclinical and clinical studies. Three-dimensional cell culture has been previously shown to support liver cells,[12] and proposed as optimal bioartificial support for progenitor and stem cells to drive differentiation towards hepatic phenotypes.[40–42]

Cells in the body are constantly exposed to biomechanical stimuli. These biomechanical stimuli regulate cell behaviour, proliferation and differentiation status and play an important role in the cellular response to molecules and drugs. Therefore, the development and application of appropriate 3D dynamic culture systems that can provide such stimuli is essential for the successful recapitulation of organ and tissue bio-engineered models. Such a technology based on stimuli-responsive materials and advanced 3D strategies has been recently described as the natural development of tissue bio-engineering, a 4D bioreactor.[43] This advanced 4D setting aims to offer dynamic 3D biological structures, instrumental to support stem cell growth and/or maturation towards target organ phenotype. 4D bioreactors can regulate biochemical variables, such as nutrient, waste and growth factor levels, and control of culture parameters over time. Furthermore, the media perfusion and the shear stress resulting from it promote the maturation of cells and tissues in vitro by enhancing nutrient and waste transportation and by providing flow-mediated mechanical stimuli.[44–46]

The nature and characteristics of the cells seeded in a 3D scaffold are essential features to be considered when generating a bioengineered liver tissue. The liver cells have been for long the elective choice, due to the swinging results reported so far using different pluripotent and multipotent stem cells to generate functional HLC. During the past years, we explored the use of a novel source of perinatal multipotent cells, AEC as a potential source for functional hepatocyte-like cells. Perinatal tissues represent a large source of non-controversial and multipotent cells.[47] Over 140 million babies are born each year globally, providing a promising source of AEC that can be isolated with modest costs for isolation and banking. In fact, the generation of human AEC lines does not require invasive or expensive procedures and is not associated with ethical controversies.[31,48] Additionally, the low expression of human leucocyte antigens (such as HLA-A, HLA-B, HLA-C and HLA-DR) in AEC can also be attributed to their immune privilege features, which suggests a potential immune tolerance after transplantation.[49,50] Previous results supported AEC engraftment once implanted in murine liver parenchyma and differentiation into functional hepatocytes, supporting applications in regenerative medicine and cell therapy.[25,47,51]

Although in vivo maturation has rescued animals with congenital or acute liver diseases, it would be relevant to produce functional HLC from AEC in vitro, to be used in disease and drug testing models as well as to perform preclinical proof-of-concept transplantation experiments in animal models and of liver-support devices. However, hepatic differentiation protocols are currently inefficient to generate HLC with fetal or adult-like characteristics from AEC cells *in vitro*. We hypothesised as a more physiological culture system enriched with ECM, such as the one offered by decellularised whole-organ, may offer support to overcome such incomplete maturation into functional HLC.[29] Therefore, in this study, we expanded and induced hepatic differentiation of human minimally manipulated AEC directly inside a 3D rat ECM whole liver scaffold. Despite being used for other stem cell types, this is the first

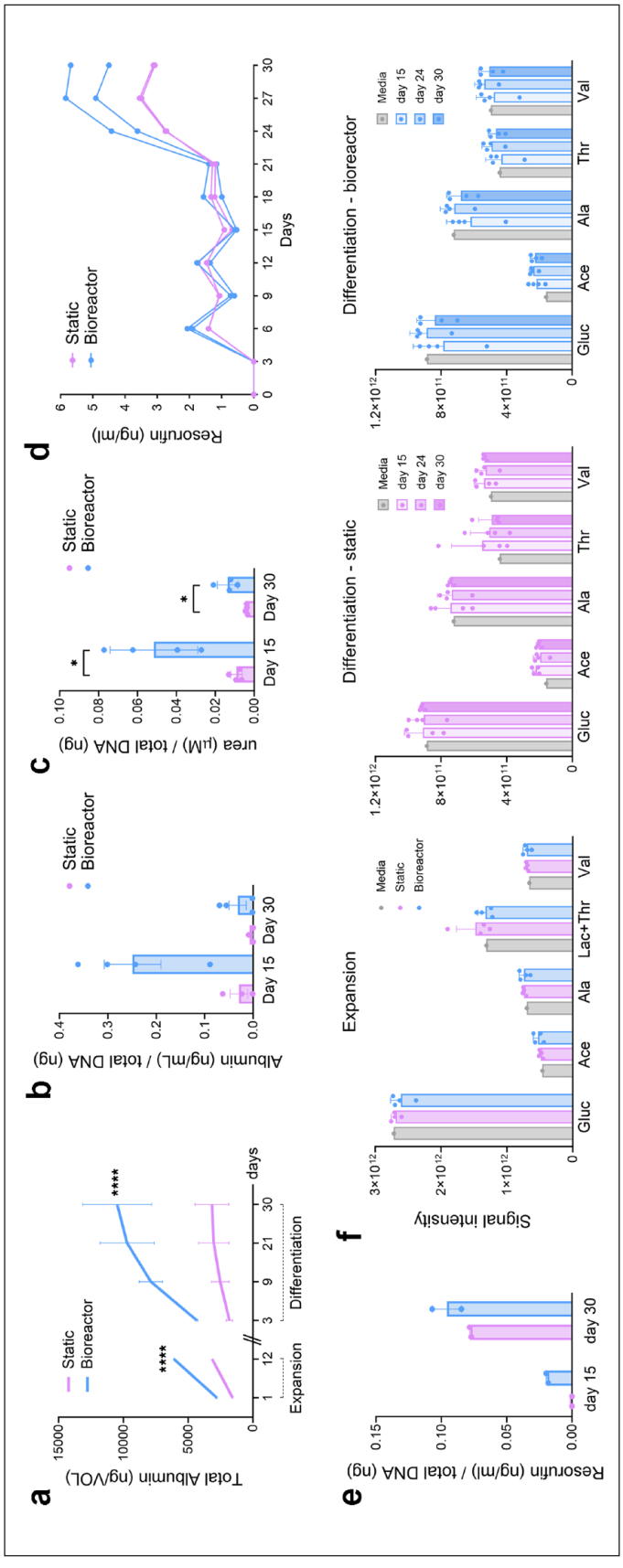

Figure 4. Functional and metabolic analysis of AEC cultured in ECM scaffolds.(a and b) quantification of albumin in culture supernatant with ELISA assay, (a) total albumin in circulation at different time points, (b) concentration of albumin normalised on the total DNA amount in each cultured scaffold collected at days 15 and 30 of culture, (c) urea concentration in culture normalised on the total DNA amount in each cultured scaffold collected at days 15 and 30 of culture ($n = 4$, mean ± SD on both graphs; a = two-way ANOVA; b, c = t-test and two-way ANOVA). (d and e) EROD assay measuring resorufin concentration in culture media post-incubation and conversion of 7-ethoxyresorufin, showing CYP1 activity in both cultured conditions over the days of differentiation only ($n = 2$ each culture condition – d) and normalised on the total DNA amount in each cultured scaffold collected at day 15 and 30 of culture (e). (f) Signal intensities of defined bins of metabolites present in cultured and control media analysed via NMR ($n = 4$, mean ± SD).

proof of principle that shows the combination of a custom perfusion bioreactor, decellularised liver-specific ECM and AEC.

In our protocol, cryopreserved AEC were initially seeded in decellularised scaffold and cultured in expansion medium for acclimatisation. The cell suspension was proved to be a homogeneous suspension of viable AEC, equipped with several epithelial-characteristic surface molecules instrumental to grant AEC adhesion to the ECM scaffold. Then, the seeded AEC were exposed to hepatic differentiation medium for additional 3 weeks. Such a protocol was performed in static condition, and with the scaffold subjected to a continuous perfusion of medium provided by a bioreactor connected to a macrofluidic system. In both conditions, immunohistological analyses proved the presence of human HLC in the scaffold with expected epithelial morphology. We detected expression of hepatic markers such as ALB, CYPs and CK18. Perinatal AEC were negative for all hepatic markers and enzymes before seeding in the liver ECM, therefore such expression was promoted by the differentiation medium and 3D culture condition in the liver ECM. Results obtained from both static and bioreactor culture conditions indicated that, in respect to inefficient approaches in 2D cultures,[21] the ECM alone was able to support differentiation towards HLC. Few AEC were still positive for AFP, a marker of fetal stages of hepatocyte development, and HNF4α, a critical hepatic mediator in liver regenerative processes. To enhance the partial hepatic differentiation offered by exogenic stimuli provided in the medium, we introduced the use of a bioreactor to support cell viability and functional improvement in rat ECM whole liver scaffolds. Bioreactors enable efficient oxygenation and exposure of nutrients to the cells by constant perfusion of media through the vasculature tree of the liver,[12] mimicking more physiological conditions. Histological analyses and total DNA quantification showed a comparable number of cells attached to the ECM of the scaffolds in the bioreactor compared to static conditions. The cells were organised in clusters, with almost no or very few cells scattered. Curiously, the comparable cell number suggested that the AEC did not seem to expand in the scaffold and that the bioreactor did not enhance scaffold repopulation in respect to static conditions. Human AEC in bioreactor condition were positive for hepatic markers (such as CK18 and ALB) and expressed lower levels of AFP compared to cells differentiated in static conditions, advocating for improved differentiation in recirculating perfusion. Mature hepatocytes are generally negative for CK19, but express keratins 8 and 18.[52,53] Co-expression of CK18 and CK19, was present in both conditions and remained higher in bioreactor conditions, supporting a limited efficiency in hepatic differentiation, but resulting in hepatic progenitor cells (bipotent hepatoblasts), with the potential to differentiate into both hepatocytes or cholangiocytes.[44,52] Additional confirmation of enhanced HLC functionality in bioreactors was offered by the detection of HNF4α. CYP3A4, the most abundant and critical cytochrome P450 enzyme in humans, normally upregulated at very late stages of hepatic development,[37,48,54,55] was present, although in low amount, in both static and dynamic conditions. CYP3A4 expression by stem cell-derived hepatocytes is considered as final proof of efficient functional improvement towards hepatocytes, emphasising the value of the ECM and 3D culture in directing cell specification.[37,56] Overall, the optimised culture condition (expansion and differentiation in 3D scaffolds in bioreactors) showed promising results, as cells displayed a hepatocyte-like morphology, phenotype and higher expression of hepatic functional markers at gene and protein levels. Gene expression analysis generally confirmed the presence of more mature HLC in scaffolds in bioreactors (as indicated by enhanced expression of *UGT1A*, *CYP3A7*, *HNF4α*, *A1AT1*, *ALB* and *AFP*). There was an obvious increase in the ratio of CYP3A4/AFP and CK18/AFP expression comparing static vs bioreactor conditions, which can indicate that the differentiation of hepatocytes is promoted by the perfusion culture. Nevertheless, in general, gene expression was lower than adult hepatocytes, indicating that full maturation of AEC into HLC was not achieved and is likely to be needing the presence of other cell types and stimuli, similarly to in vivo. It would be interesting in future to test whether the addition of other cells, for example endothelial cells or hepatic stellate cells, is able to further promote hepatocyte differentiation and maturation in the 3D culture system supported by the bioreactor.[57–60]

The significant increase in hepatic secretion (albumin release) and metabolism (urea production) during the differentiation step inside the bioreactor and during the time of the culture supports an enhanced ex vivo functional improvement of human perinatal cells.[61] As a further evaluation of AEC-derived HLC functionality, we measured CYP1A1 function via EROD assay, as regularly measured in human hepatocytes.[21] AEC-derived HLCs were found active in CYP1A1 activity from day 6 of the differentiation protocol. The activity fluctuated over the 30 days of differentiation, but increased steadily between days 21 and 27. Of note, rifampicin, a potent CYP-inducer,[62] was added to the differentiation media from day 10 of differentiation. CYP1A1 activity was found diminishing in the last 3 days of culture, confirming a clear decrease in HLC functionality also shown by a decreased albumin and urea production over days 27–30. Overall CYP functionality was found enhanced in HLC cultured in scaffolds in the bioreactor, compared to static conditions, and we hypothesised such improvement is a consequence of more efficient oxygenation and perfusion achieved with the use of the bioreactor, which maximises the exposure of the cells to nutrients in the media.[12] Metabolite analysis in the cultured media via

NMR did not indicate substantial changes among conditions, possibly due to cells to media ratio. Of note, cells in 3D culture in the bioreactor seemed to consume glucose at early time points and showed a shift in metabolite profile around day 24, similarly to trends determined for albumin and EROD assays. Take together, these results indicate that AEC differentiation into HLC reached best performance between 24 and 27 days of differentiation, which will probably produce the best cell performance in future experiments.

Human AEC are a promising source of cells with several advantages over other sources of stem cells for generating bioengineered livers. Amnion cells have been previously used in several studies to generate hepatocytes in vitro using different protocols and conditions. Despite the promising progress in obtaining AEC-derived hepatocytes, all the studies showed limited metabolic activity, which was found similar to fetal liver and not fully representative of mature liver functions. AEC-derived hepatocytes showed enhanced hepatic phenotype and functionality, comparable to mature liver, only upon transplantation in vivo functions.[25,29,63] Here, we confirmed that advanced 3D culture systems that include rat ECM whole liver scaffolds and continuous perfusion of media via bioreactor culture can improve hepatic differentiation compared to previous studies in vitro. In addition to the role of the bioreactor, the preserved ECM components in the decellularised liver scaffolds may have a considerable role in the improvement of differentiation, providing crucial cues for main cellular behaviour such as proliferation and differentiation by ECM-cell interactions.[64] Interestingly, AEC have been successfully differentiated into hepatic sinusoid endothelial cells by Serra et al.,[65] which suggests the potential to exploit these cells to level up the bioengineered liver constructs even further in the future, potentially generating a multi-cellular liver construct.

Conclusions

Perinatal epithelial cells paving the amnion membrane are multipotent cells, easily and safely collected at the end of any pregnancy. Such fetal-derived perinatal cells can be used in regenerative medicine because of their differentiation potential, genetic stability and immunomodulatory properties. 3D decellularised rat liver scaffolds were successfully generated and used to promote the ability of AEC to differentiate into functional hepatocytes. We successfully optimised the culture condition of AEC in 3D decellularised liver scaffolds; a considerable improvement was noted in homing and differentiation of cells expanded in 3D and cultured using a bioreactor, compared to static culture conditions. Further analyses are needed to confirm the differentiation status of AEC, but preliminary data obtained are supporting AEC capability of generating functional hepatocyte-like cells in vitro, supporting the use of dynamic bioreactor-based systems to enhance the differentiation of progenitor cells. The same approach may be used to test whether the bioreactor system combined with tissue-specific ECM extracts is able to aid the differentiation of pluripotent stem cells (i.e. iPSCs and ESCs) towards functional human hepatocytes which, to date, is still non-satisfactory. Therefore, the approach here proposed could overcome the limitations and obstacles associated with the use of pluripotent stem cells in liver regenerative medicine.

Acknowledgements

We would like to thank Prof Ajay Shah and Dr Anna Zoccarato (King's College London) for the donation of rat liver for the project. We thank the Centre for Biomolecular Spectroscopy, Randall Centre for Cell and Molecular Biophysics, Kings College London, funded by the Wellcome Trust and British Heart Foundation (ref. 202767/Z/16/Z and IG/16/2/32273), including Drs James Jarvis (NMR Facility). We also thank George Chennell and Chen Liang (Facility Manager at Wohl Cellular Imaging Centre King's College London) for helping with confocal image acquisition. We are grateful to Prof Shilpa Chokshi for the useful discussion.

Author contributions

Conceptualization: LU and RG. Methodology: SC, BA, NG and LU. Investigation: SC, BA, NG performed seeding experiments and subsequent analysis, including immunofluorescence and image analysis, ELISA tests, mycoplasma test, EROD assay. FGF performed image processing and quantification analysis. CMQ performed the characterisation of rat liver scaffolds. VK, GG and SB performed RNA extraction and qPCR analysis. JC performed NMR analysis. ALG acquired NMR data. DN performed preliminary experiments to support the study. Formal analysis: SC, BA, SB. Resources: LU and RG. Writing – Original Draft: SC, LU, BA and RG. Writing – Review & Editing: SC, LU, BA and RG. Visualization: SC and LU. Supervision, Project administration and funding acquisition: LU and RG.

Availability of data and materials

The data used and/or analysed during the current study are available from the corresponding author on reasonable request.

Declaration of conflicting interests

The author(s) declared no potential conflicts of interest with respect to the research, authorship, and/or publication of this article.

Funding

The author(s) disclosed receipt of the following financial support for the research, authorship, and/or publication of this article: This work was supported by Åke Wibergs stiftelse (RG) and the Foundation for Liver Research (LU and team and IJC).

Ethics approval and consent to participate

Human placentae were collected from full-term healthy pregnancies at Karolinska Hospital (Stockholm, Sweden) at the end of uncomplicated caesarean resection procedures. The placenta was received within 90 min after delivery at the Karolinska Institute laboratory, as detailed in approved ethical permit (nr. 2015/419-34/4), and upon parental informed consent.

ORCID iDs

Luca Urbani https://orcid.org/0000-0002-4988-552X

Supplemental material

Supplemental material for this article is available online.

References

1. Mokdad AA, Lopez AD, Shahraz S, et al. Liver cirrhosis mortality in 187 countries between 1980 and 2010: a systematic analysis. *BMC Med* 2014; 12(1): 145.
2. Asrani SK, Devarbhavi H, Eaton J, et al. Burden of liver diseases in the world. *J Hepatol* 2019; 70(1): 151–171.
3. Dutkowski P, Oberkofler CE, Béchir M, et al. The model for end-stage liver disease allocation system for liver transplantation saves lives, but increases morbidity and cost: a prospective outcome analysis. *Liver Transpl* 2011; 17(6): 674–684.
4. Furuta T, Furuya K, Zheng Y-W, et al. Novel alternative transplantation therapy for orthotopic liver transplantation in liver failure: a systematic review. *World J Transplant* 2020; 10(3): 64–78.
5. Dhawan A. Clinical human hepatocyte transplantation: current status and challenges. *Liver Transpl* 2015; 21 Suppl 1: S39–S44.
6. Rotolo A, Chabannon C and Gramignoli R. Identification of hurdles in the development of cell-based therapies. *Cytotherapy* 2020; 22(2): 53–56.
7. Adam R, Karam V, Cailliez V, et al. 2018 annual report of the European liver transplant registry (ELTR) – 50-year evolution of liver transplantation. *Transpl Int* 2018; 31(12): 1293–1317.
8. Vishwakarma SK, Lakkireddy C, Bardia A, et al. Bioengineered functional humanized livers: an emerging supportive modality to bridge the gap of organ transplantation for management of end-stage liver diseases. *World J Hepatol* 2018; 10(11): 822–836.
9. Hynes Ro. The extracellular matrix: not just pretty fibrils. *Science* 2009; 326(5957): 1216–1219.
10. McCrary MM, Bousalis D, Mobini S, et al. Decellularized tissues as platforms for in vitro modeling of healthy and diseased tissues. *Acta Biomater* 2020; 111: 1–19.
11. Maghsoudlou P, Georgiades F, Smith H, et al. Optimization of liver decellularization maintains extracellular matrix micro-architecture and composition predisposing to effective cell seeding. *PLoS One* 2016; 11(5): e0155324.
12. Sassi L, Ajayi O, Campinoti S, et al. A perfusion bioreactor for longitudinal monitoring of bioengineered liver constructs. *Nanomaterials* 2021; 11(2): 275.
13. Acun A, Oganesyan R, Jaramillo M, et al. Human-origin iPSC-based recellularization of decellularized whole rat livers. *Bioengineering* 2022; 9(5): 219.
14. Carpentier N, Urbani L, Dubruel P, et al. The native liver as inspiration to create superior in vitro hepatic models. *Biomater Sci* 2023; 11(4): 1091–1115.
15. Chen Y, Geerts S, Jaramillo M, et al. Preparation of decellularized liver scaffolds and recellularized liver grafts. *Methods Mol Biol* 2018; 1577: 255–270.
16. Antarianto RD, Pragiwaksana A, Septiana WL, et al. Hepatocyte differentiation from iPSCs or MSCs in decellularized liver scaffold: cell-ECM adhesion, spatial distribution, and hepatocyte maturation profile. *Organogenesis* 2022; 18(1): 2061263.
17. Baptista PM, Siddiqui MM, Lozier G, et al. The use of whole organ decellularization for the generation of a vascularized liver organoid. *Hepatology* 2011; 53(2): 604–617.
18. Hoyle HW, Stenger CML and Przyborski SA. Design considerations of benchtop fluid flow bioreactors for bio-engineered tissue equivalents in vitro. *Biomater Biosyst* 2022; 8: 100063.
19. Juste-Lanas Y, Hervas-Raluy S, García-Aznar JM, et al. Fluid flow to mimic organ function in 3D in vitro models. *APL Bioeng* 2023; 7(3): 031501.
20. Yamada S, Yassin MA, Schwarz T, et al. Optimization and validation of a custom-designed perfusion bioreactor for bone tissue engineering: flow assessment and optimal culture environmental conditions. *Front Bioeng Biotechnol* 2022; 10: 811942.
21. Gramignoli R, Tahan V, Dorko K, et al. Rapid and sensitive assessment of human hepatocyte functions. *Cell Transplant* 2014; 23(12): 1545–1556.
22. Ang LT, Tan AKY, Autio MI, et al. A roadmap for human liver differentiation from pluripotent stem cells. *Cell Rep* 2018; 22(8): 2190–2205.
23. Cross JC. Formation of the placenta and extraembryonic membranes. *Ann N Y Acad Sci* 1998; 857: 23–32.
24. Antoniadou E and David AL. Placental stem cells. *Best Pract Res Clin Obstet Gynaecol* 2016; 31: 13–29.
25. Marongiu F, Gramignoli R, Dorko K, et al. Hepatic differentiation of amniotic epithelial cells. *Hepatology* 2011; 53(5): 1719–1729.
26. Ilancheran S, Moodley Y and Manuelpillai U. Human fetal membranes: a source of stem cells for tissue regeneration and repair? *Placenta* 2009; 30(1): 2–10.
27. Skvorak KJ, Dorko K, Marongiu F, et al. Improved amino acid, bioenergetic metabolite and neurotransmitter profiles following human amnion epithelial cell transplant in intermediate maple syrup urine disease mice. *Mol Genet Metab* 2013; 109(2): 132–138.
28. Skvorak KJ, Dorko K, Marongiu F, et al. Placental stem cell correction of murine intermediate maple syrup urine disease. *Hepatology* 2013; 57(3): 1017–1023.
29. Lin JS, Zhou L, Sagayaraj A, et al. Hepatic differentiation of human amniotic epithelial cells and in vivo therapeutic effect on animal model of cirrhosis. *J Gastroenterol Hepatol* 2015; 30(11): 1673–1682.
30. Gramignoli R, Srinivasan RC, Kannisto K, et al. Isolation of human amnion epithelial cells according to current good manufacturing procedures. *Curr Protoc Stem Cell Biol* 2016; 37: 1e.10.1–1e.10.13.
31. Miki T, Marongiu F, Ellis R, et al. Isolation of amniotic epithelial stem cells. *Curr Protoc Stem Cell Biol* 2007; Chapter 1: Unit 1E.3.

32. Tchoukalova YD, Zacharias SRC, Mitchell N, et al. Human amniotic epithelial cell transplantation improves scar remodeling in a rabbit model of acute vocal fold injury: a pilot study. *Stem Cell Res Ther* 2022; 13(1): 31.
33. Srinivasan RC, Strom SC and Gramignoli R. Effects of cryogenic storage on human amnion epithelial cells. *Cells* 2020; 9(7): 1696.
34. Morandi F, Marimpietri D, Görgens A, et al. Human amnion epithelial cells impair T cell proliferation: the role of HLA-G and HLA-E molecules. *Cells* 2020; 9(9): 2123.
35. Pang Z, Chong J, Zhou G, et al. MetaboAnalyst 5.0: narrowing the gap between raw spectra and functional insights. *Nucleic Acids Res* 2021; 49(W1): W388–W396.
36. Fanti M, Gramignoli R, Serra M, et al. Differentiation of amniotic epithelial cells into various liver cell types and potential therapeutic applications. *Placenta* 2017; 59: 139–145.
37. Miki T, Lehmann T, Cai H, et al. Stem cell characteristics of amniotic epithelial cells. *Stem Cells* 2005; 23(10): 1549–1559.
38. Baxter M, Withey S, Harrison S, et al. Phenotypic and functional analyses show stem cell-derived hepatocyte-like cells better mimic fetal rather than adult hepatocytes. *J Hepatol* 2015; 62(3): 581–589.
39. Raju R, Chau D, Notelaers T, et al. In vitro pluripotent stem cell differentiation to hepatocyte ceases further maturation at an equivalent stage of E15 in mouse embryonic liver development. *Stem Cells Dev* 2018; 27(13): 910–921.
40. Dai Q, Jiang W, Huang F, et al. Recent advances in liver engineering with decellularized scaffold. *Front Bioeng Biotechnol* 2022; 10: 831477.
41. Hosseini V, Maroufi NF, Saghati S, et al. Current progress in hepatic tissue regeneration by tissue engineering. *J Transl Med* 2019; 17(1): 383.
42. Toprakhisar B, Verfaillie CM and Kumar M. Advances in recellularization of decellularized liver grafts with different liver (stem) cells: towards clinical applications. *Cells* 2023; 12(2): 301.
43. Li YC, Zhang YS, Akpek A, et al. 4D bioprinting: the next-generation technology for biofabrication enabled by stimuli-responsive materials. *Biofabrication* 2016; 9(1): 012001.
44. Freyer N, Knöspel F, Strahl N, et al. Hepatic differentiation of human induced pluripotent stem cells in a perfused three-dimensional multicompartment bioreactor. *Biores Open Access* 2016; 5(1): 235–248.
45. Xie Y, Yao J, Jin W, et al. Induction and maturation of hepatocyte-like cells in vitro: focus on technological advances and challenges. *Front Cell Dev Biol* 2021; 9: 765980.
46. Huang X, Huang Z, Gao W, et al. Current advances in 3D dynamic cell culture systems. *Gels* 2022; 8(12): 829.
47. Zhang Q and Lai D. Application of human amniotic epithelial cells in regenerative medicine: a systematic review. *Stem Cell Res Ther* 2020; 11(1): 439.
48. Miki T, Marongiu F, Ellis EC, et al. Production of hepatocyte-like cells from human amnion. *Methods Mol Biol* 2009; 481: 155–168.
49. Hammer A, Hutter H, Blaschitz A, et al. Amnion epithelial cells, in contrast to trophoblast cells, express all classical HLA class I molecules together with HLA-G. *Am J Reprod Immunol* 1997; 37(2): 161–171.
50. Akle CA, Adinolfi M, Welsh KI, et al. Immunogenicity of human amniotic epithelial cells after transplantation into volunteers. *Lancet* 1981; 2(8254): 1003–1005.
51. Miki T. Amnion-derived stem cells: in quest of clinical applications. *Stem Cell Res Ther* 2011; 2(3): 25.
52. Miki T, Ring A and Gerlach J. Hepatic differentiation of human embryonic stem cells is promoted by three-dimensional dynamic perfusion culture conditions. *Tissue Eng Part C Methods* 2011; 17(5): 557–568.
53. Yang L, Wang WH, Qiu WL, et al. A single-cell transcriptomic analysis reveals precise pathways and regulatory mechanisms underlying hepatoblast differentiation. *Hepatology* 2017; 66(5): 1387–1401.
54. Park HJ, Choi YJ, Kim JW, et al. Differences in the epigenetic regulation of cytochrome P450 genes between human embryonic stem cell-derived hepatocytes and primary hepatocytes. *PLoS One* 2015; 10(7): e0132992.
55. Schuetz JD, Beach DL and Guzelian PS. Selective expression of cytochrome P450 CYP3A mRNAs in embryonic and adult human liver. *Pharmacogenetics* 1994; 4(1): 11–20.
56. Ong SY, Dai H and Leong KW. Inducing hepatic differentiation of human mesenchymal stem cells in pellet culture. *Biomaterials* 2006; 27(22): 4087–4097.
57. Ardalani H, Sengupta S, Harms V, et al. 3-D culture and endothelial cells improve maturity of human pluripotent stem cell-derived hepatocytes. *Acta Biomater* 2019; 95: 371–381.
58. Takebe T, Zhang RR, Koike H, et al. Generation of a vascularized and functional human liver from an iPSC-derived organ bud transplant. *Nat Protoc* 2014; 9(2): 396–409.
59. Ramachandran SD, Schirmer K, Münst B, et al. In vitro generation of functional liver organoid-like structures using adult human cells. *PLoS One* 2015; 10(10): e0139345.
60. Ware BR, Durham MJ, Monckton CP, et al. A cell culture platform to maintain long-term phenotype of primary human hepatocytes and endothelial cells. *Cell Mol Gastroenterol Hepatol* 2018; 5(3): 187–207.
61. Chaudhari P, Tian L, Deshmukh A, et al. Expression kinetics of hepatic progenitor markers in cellular models of human liver development recapitulating hepatocyte and biliary cell fate commitment. *Exp Biol Med* 2016; 241(15): 1653–1662.
62. Chen J and Raymond K. Roles of rifampicin in drug-drug interactions: underlying molecular mechanisms involving the nuclear pregnane X receptor. *Ann Clin Microbiol Antimicrob* 2006; 5: 3.
63. Maymó JL, Riedel R, Pérez-Pérez A, et al. Proliferation and survival of human amniotic epithelial cells during their hepatic differentiation. *PLoS One* 2018; 13(1): e0191489.
64. Debnath T, Mallarpu CS and Chelluri LK. Development of bioengineered organ using biological acellular rat liver scaffold and hepatocytes. *Organogenesis* 2020; 16(2): 61–72.
65. Serra M, Marongiu M, Contini A, et al. Evidence of amniotic epithelial cell differentiation toward hepatic sinusoidal endothelial cells. *Cell Transplant* 2018; 27(1): 23–30.